Intravascular arrest of circulating tumor cells is a two-step process exploiting their adhesion repertoire.

Naël Osmani[1-4*], Gautier Follain[1-4*], Maria Jesus Garcia-Leon[1-4], Olivier Lefebvre[1-4], Sébastien Harlepp[1-5], Jacky G. Goetz[1-5]

[1] INSERM UMR_S1109, Strasbourg, F-67000, France.
[2] Université de Strasbourg, Strasbourg, F-67000, France.
[3] LabEx Medalis, Université de Strasbourg, Strasbourg, F-67000, France.
[4] Fédération de Médecine Translationnelle de Strasbourg (FMTS), Strasbourg, F-67000, France.
[5] Corresponding author

[*] These authors contributed equally to this work

Materials and correspondance, *lead author:
Jacky G. GOETZ*, jacky.goetz@inserm.fr, Sébastien HARLEPP, harlepp@unistra.fr
INSERM UMR_S1109, 67000 Strasbourg, France; Fédération de Médecine Translationnelle de Strasbourg (FMTS), 67000 Strasbourg, France
Web: www.goetzlab.com, twitter: @GoetzJacky

Keywords:
Circulating tumor cell, arrest, adhesion, metastasis, biomechanics zebrafish

ABSTRACT

Cancer metastasis is a process in which a primary tumor spreads to form life-threatening metastases. Circulating tumor cells (CTCs) may arrest in distant organs and escape by crossing the endothelial barrier. We have previously demonstrated that blood flow controls sequential CTC arrest and stable adhesion to endothelial cells. We now aim at identifying the adhesion receptors involved in each step. Early arrest is mediated by the formation of adhesion of weak magnitude of forces depending on CD44 and integrin αvβ3. Stabilization of this arrest uses integrin α5β1 dependent adhesions with larger magnitude of forces, which allows arrested CTCs to resist the shear forces conveyed by the blood flow. Finally, blood flow favors luminal deposition of fibronectin by endothelial cells, an integrin α5β1 ligand. In conclusion, we identified the molecular partners that are sequentially exploited by CTCs to arrest in vascular regions with permissive flow regimes, before extravasation.

INTRODUCTION

Cancer metastasis is a complex multi-step process in which secondary tumors are formed at distant organs ultimately leading to the death of patients. After escaping the primary tumor, cancer cells invade the surrounding stroma and reach vessels, where they enter blood or lymph circulation. Once in the blood flow, circulating tumor cells (CTCs) may reach distant organs, where they will extravasate from the blood circulation and either remain dormant or form new tumor foci (Obenauf and Massagué, 2015). Several recent studies suggest that most metastases are formed from cancer cells that disseminate efficiently and very early during cancer progression (Eyles et al., 2010; Harper et al., 2016; Hosseini et al., 2016; Rhim et al., 2012). Over the past two decades, extensive work has been achieved to study the molecular receptors potentially involved in the intravascular adhesion of CTCs to the endothelium (Reymond et al., 2013). In particular, glycoproteins involved in the rolling of leukocytes at the surface of the endothelium have been widely studied. For example, selectins present on the endothelium are required for the adhesion of colon or breast cancer cells to endothelial cells (Aigner et al., 1998; Laferrière et al., 2001). At the surface of tumors cells, glycoprotein such as CD24, CD44, PODXL and mucins were shown to mediate CTC adhesion to the endothelium (Aigner et al., 1998; Dallas et al., 2012; Hanley et al., 2006; Rahn et al., 2005; Shea et al., 2015). Finally, *in vitro* studies using different cancer cell lines have shown the requirement of

the integrin family of adhesion receptors at the surface of CTCs for their arrest and adhesion to endothelial cells. More specifically, integrins αvβ3 and β1 have been involved in breast and prostate cancer cells (Barthel et al., 2013; Felding-Habermann et al., 2001; Reymond et al., 2012), β4 in prostate and colon cancer derived cell line (Barthel et al., 2013; Laferrière et al., 2004) and α4β1 in melanoma (Klemke et al., 2007). However, the respective contribution of these receptors in CTC arrest and adhesion remains elusive. Furthermore, while there is an extensive amount of studies performed *in vitro*, very little information on how these receptors are recruited and used in a realistic *in vivo* situation is available. Recently, using a combination of easy-to-tune microfluidics as well as intravital imaging in two animal models, we have shown that blood flow tunes CTC arrest, preceding metastatic outgrowth (Follain et al., 2018a). We showed that shear forces compete with the adhesion potential of CTCs, through a tug of war, and thereby control their probability of intravascular arrest. Using the zebrafish embryo, we observed that CTC arrest immediately after the entry within the blood circulation between 0 and 5 minutes post-injection (mpi) and that cells may still be detached from the endothelium by blood shear stress. Then, CTCs form stable adhesion between 1 and 3 hours post-injection (hpi) that prevents them from shear-mediated detachment. This suggests that CTCs may use two consecutive steps very likely molecularly mediated by different adhesion receptors. Studies from the molecular mechanisms engaged by leukocytes during intravascular arrest is driven by adhesions of weak forces mediated by receptors such as CD44 while stable adhesion depends on integrin-dependent adhesions (Eibl et al., 2012; McEver and Zhu, 2010).

Here, we demonstrate that arrest of CTC is driven by two major steps: (i) early arrest mediated by the formation of *de novo* adhesions of weak magnitude of forces and (ii) the stabilization of CTC/endothelium adhesions through the recruitment of adhesions with larger magnitude of forces. Altogether, these 2 consecutive steps allow arrested CTCs to resist the shear stress from the blood flow. At a molecular level, the glycoprotein CD44 and the integrin αvβ3 are required for early metastable adhesion to endothelial cells. In contrast, integrin α5β1 is later required to strengthen intravascular arrest through stable adhesions. Finally, we observe that endothelial cells subjected to flow profiles that are permissive for intravascular arrest and extravasation secrete more fibronectin, a major ligand of integrins αvβ3 and α5β1, on their luminal side.

RESULTS

CD44, ITGB3 and ITGB1 favor arrest and adhesion of CTCs, yet only ITGB1 is required for stable adhesion to the endothelial layer

In order to assess the role of adhesion receptors of weak and larger forces respectively, we decided to test the role of CD44, ITGB3 and ITGB1 in CTC arrest and adhesion (Baccelli et al., 2013; Barthel et al., 2013; Felding-Habermann et al., 2001; Reymond et al., 2012) using microfluidics (Fig. 1A). Using transient siRNA depletion, we efficiently knocked-down the expression of these cell adhesion receptors into D2A1 murine carcinoma cells (Fig. 1D and S1). We previously showed that CTC arrest is tuned by blood flow in a tug of war between CTC adhesion and blood shear forces. We identified a threshold flow value of 400~500 µm/s above which CTC adhesion is prevented (Follain et al., 2018a). We thus perfused cells into microchannels, where a confluent monolayer of HUVEC endothelial cell had been grown, and interrogated the strengthening of the adhesion between CTCs and the endothelial cells using an innovative, yet simple, experimental workflow described in Fig.1C. Briefly, we perfused CTCs and decreased velocities from 400 µm/s to 100 µm/s for 2 min for each perfusion step while live recording CTC arrest/adhesion (Fig. 1A,D, Movie 1). As expected, such decrease favored CTC adhesion (Fig. 1E, Movie 2-3). Strength of this early adhesion was then interrogated by increasing shear forces (400 µm/s) (Fig. 1A,C, Movie 1). Based on this approach, we measured that ~80% of arrested CTCs had formed stable adhesion with the endothelial layer (Fig. 1E). Interestingly, while depleting CD44, ITGB3 or ITGB1 compromised CTC early adhesion (Fig. 1E, Movie 2-3), only ITGB1 depletion impacted CTC stable adhesion to the endothelial layer (Fig. 1E).

To further interrogate the adhesion forces mediated by CD44, ITGB3 and ITGB1, we perfused D2A1 cells transfected with control or anti-CD44, ITGB3 or ITGB1 siRNAs and assessed their adhesive potential using optical tweezing. Upon adhesion of perfused D2A1 (5 min, no flow), we rapidly trapped attached CTCs and mechanically detached them from the endothelial monolayer (Fig. 1F). Identically to our live *in vitro* adhesion assay, ~80% of cells formed stable adhesion with the endothelial monolayer in control conditions. Stable adhesion was not impaired when depleting CD44, nor ITGB3, while it was significantly impacted by ITGB1 depletion (Fig 1G, Movie 4-6).

Altogether, these results suggest that CD44, ITGB3 and ITGB1 both favor the initial arrest and adhesion of CTCs, but that only ITGB1 is capable of mediating stable shear-protected adhesion of CTCs to the endothelium.

CD44 and ITGB3 are required for CTC arrest *in vivo*, only ITGB1 further stabilizes adhesion to the endothelium

It appeared that decoupling early arrest from adhesion was difficult in an *in vitro* setup. Thus, in order to study the involvement of CD44, ITGB3 and ITGB1 in CTC arrest and early adhesion, we took advantage of our well-established CTC live injection protocol using zebrafish embryo stably expressing an endothelium-specific EGFP (*Tg(Fli1a:EGFP)*) at 2 days post-fertilization (dpf) (Follain et al., 2018b). We injected fluorescently-tagged D2A1 cells that were transfected with either control siRNAs or siRNAs targeting endogenous CD44, ITGB3 or ITGB1. Upon injection, their arrest was monitored using instantaneous live imaging for 5 minutes. Such innovative experimental set-up is perfectly suited for interrogating the very early dynamics of arrest of CTCs (Fig. 2A). While the depletion of CD44 and ITGB3 impacted CTC arrest and early adhesion to the endothelium, ITGB1 depletion had no effect and CTCs arrested similarly the the arterio-venous junction (Fig. 2B-C, Movie 7-9). Accurate analysis of the dynamic behavior of CTCs in the blood flow showed that control cells had arrest time exceeding 2 minutes. CD44- and ITGB3-depleted cells were either unable to arrest or had shorter arresting time (Fig. 2C) suggesting decreased adhesive abilities. To test the involvement of CD44, ITGB3 and ITGB1 in the formation of stable adhesion to the endothelium, we assessed the number and location of adhered CTCs 3 hpi using a cumulative heatmapping protocol in a large number of *Tg(Fli1a:EGFP)* embryos (Fig. 1A) as previously described (Follain et al., 2018b). Depletion of CD44 or ITGB3 did not affect the number of cells adhered in the AVJ. On the contrary, ITGB1 depletion drastically reduced the number of cells stably arrested in the AVJ at 3hpi (Fig. 2E-G).

These data indicate that CD44/ITGB3 and ITGB1 are sequentially exploited by CTCs to mediate stable intravascular arrest *in vivo*. While CD44 and ITGB3 are required initially to mediated the first steps of CTC arrest, ITGB1 is required for strengthening and stabilizing the adhesion of CTCs that are now resistant to ripping shear forces.

Integrin α5β1 is required for the stable adhesion of CTCs to the endothelium

Integrins are heterodimers consisting of 2 subunits (α and β) which tune their ligand affinity (Campbell and Humphries, 2011). ITGB3 essentially associates to ITGAV to form the heterodimer αvβ3 which binds fibronectin and vitronectin (Humphries, 2006). ITGB1 can dimerize with several different α subunits to constitutes integrin heterodimers with very different ligand specificity (Humphries, 2006). In order to identify the subunit that, when associated to ITGB1, mediates stable adhesion of CTCs, (and thereby identify the ligand), we knocked down different integrin alpha subunits (Fig. 3A), among which integrin α4 (ITGA4), which associates to ITGB1 to interact with VCAM at the surface of the endothelium (Klemke et al., 2007), integrin α3 (ITGA3) which combines with ITGB1 to engage laminin below the endothelial layer (Chen et al., 2016a) and integrin α5 (ITGA5) which heterodimerizes with ITGB1 and binds fibronectin (Huveneers et al., 2008). We then tested their role in CTC adhesion *in vitro*, using our microfluidic live imaging assay, or *in vivo,* using intravascular injection in zebrafish embryos. We observed that ITGA4 was not involved in CTC adhesion, neither *in vitro* nor *in vivo*, suggesting no requirement of endothelial VCAM (Fig. 3B,E). Interestingly, we observed that ITGA3 mediated CTC arrest/adhesion *in vitro* as we measured a significant decrease in the number of cells attached to the endothelial layer after the perfusion steps. However, ITGA3 was not required for the formation of stable cell adhesion to the endothelial layer as siITGA3 depleted cells were insensitive to the washing step (Fig. 3C). This was further supported by the observation that ITGA3 knock down did not affect stable arrest of CTCs in the zebrafish embryo (Fig. 3F). Finally, we observed that ITGA5 depletion impaired CTC attachment and the formation of stable adhesion *in vitro* (Fig. 3D). This was further confirmed *in vivo*, where ITGA5-depleted cells were less prone to arrest in the AVJ (Fig. 3G). All in all, depletion of ITGA5 phenocopied ITGB1 depletion suggesting that the integrin α5β1 is the major mediator of stable CTC adhesion to the endothelium. Such observation further suggests that fibronectin, its main ligand, may also be involved in stabilizing intravascular arrest of CTCs.

Blood flow controls endothelial secretion of luminal fibronectin

Since we observed that integrin α5β1 is one of the main mediators of CTC stable adhesion to the endothelium, we tested the presence of fibronectin on the surface of confluent monolayers of HUVEC. Using immunostaining and 3D confocal imaging, we observed fibronectin deposits at the surface of endothelial cells which we

correspond to the luminal side of blood vessels (Fig. 4A). We have shown recently that blood flow is a major regulator of the arrest, adhesion and extravasation of CTCs. In particular, we have shown that the endothelium is sensitive to blood flow and its response to shear stress was driving endothelium remodeling to promote CTC extravasation (Follain et al., 2018a). We thus explored the hypothesis that flow might directly tune CTC adhesion to the endothelium from an endothelial standpoint. We thus wondered whether flow might control the formation of fibronectin deposits on the luminal side which would cooperate with the flow-mediated adhesive capacities of CTCs to favor the creation of an adhesion favorable platform on the lumen of blood vessels.

To do so, we cultured HUVEC cells in microfluidic channels and subjected to absence of flow or imposed flow of 400 µm/s (*i.e.* flow velocity that is permissive to arrest and extravasation *in vivo* (Follain et al., 2018a). We observed that endothelial cells subjected to flow had a 4,8-fold increase in luminal fibronectin compared to cells cultured without flow (Fig. 4A-B). Remarkably, we did not observe any flow-dependent effect on fibronectin expression in HUVEC cells by western blot (Fig. 4C). This suggests that flow might favor the secretion of endothelial fibronectin as previously shown for TRPV4 ion channel (Baratchi et al., 2016). We then performed immunostaining for endogenous fibronectin in *Tg(Fli1a:EGFP)*) embryos at 2 days post-fertilization and observed luminal fibronectin in the caudal plexus as well as in the inter somitic vessels (ISVs – Fig. 4F). Remarkably, we observed increased deposition of fibronectin in the dorsal aorta (DA), where the blood flow velocity is higher than in the AVJ (Fig. 4F). To further investigate the role of blood flow on the presence of luminal fibronectin, we pharmacologically decreased blood flow profiles by incubating them in lidocaine (Follain et al., 2018a). Reducing blood flow velocities led to a significant decrease in the number of embryos with fibronectin deposits.

Altogether, these observations suggest that blood flow also tunes indirectly CTC arrest and adhesion by the deposition of fibronectin at the surface of blood vessels, which act as major adhesion scaffold. In conclusion, blood flow synergistically controls the efficient intravascular arrest of CTCs: it favors arrest of CTCs which cannot sustain shear ripping forces and it induces the deposition of fibronectin that is later exploited for stabilizing the adhesion of CTCs, preceding metastatic outgrowth.

DISCUSSION

Using live intravital imaging in the zebrafish embryo, we recently documented that CTC adhesion is a multi-step process which requires (i) their arrest shortly after their entry into the blood circulation by direct interaction with the endothelial layer and (ii) the stabilization of CTC-endothelium interaction through the formation of stable adhesions whose forces exceed the local shear stress exerted by the blood flow for successful extravasation (Follain et al., 2018a). Furthermore, we have shown that blood flow tunes CTC arrest by a process which is encoded into a tug-of-war between blood flow-driven shear stress and the limited adhesive power of a single CTCs in suspension (Figure 1A). CTC adhesion to the endothelium, preceding their exit of the blood stream, has been extensively studied either *in vitro* (Aigner et al., 1998; Chen et al., 2016a; Giavazzi et al., 1993a; Laferrière et al., 2001, 2004; Reymond et al., 2012; Tremblay et al., 2008) or *in vivo* (Hiratsuka et al., 2011; Köhler et al., 2010; Stoletov et al., 2010) for the past 30 years, giving a general idea of which adhesion receptors might be involved in such events. However, no study so far could detail at high spatio-temporal resolution the events leading to CTC arrest and the respective contributions of adhesion receptors. Thus, the influence of low force adhesion receptors versus high force adhesion receptors in CTC arrest and adhesion to the endothelium remains elusive.

In the present work, we exploited the multiple advantages of combined microfluidics and experiments conducted in vivo in zebrafish embryo to provide an original description of CTC arrest. We report that early arrest is mediated by CD44 and integrin αvβ3, both being reported as receptors of weak magnitude of forces (Bano et al., 2016). Indeed, CD44 has been involved in the rolling of leukocytes along the endothelium and is found expressed in breast cancer CTCs with higher metastatic potential (Baccelli et al., 2013; Boral et al., 2017). Integrin αvβ3, a major fibronectin ligand, has been suggested to mediate weaker adhesion involved in mechanosensing during cell migration over a matrix of fibronectin (Roca-Cusachs et al., 2009; Bharadwaj et al., 2017). We also show that CTC/endothelium bonds are quickly stabilized to resist the shear stress from the blood flow with the formation of integrin α5β1 dependent adhesions. These integrin α5β1 adhesions have been shown to be involved in the formation of more stable adhesions, in cells migrating over a matrix of fibronectin by producing larger magnitude of bonding forces than integrin αvβ3 (Roca-Cusachs et al., 2009; Kong et al., 2009, 2013; Bharadwaj et al., 2017).

Several studies *in vitro* or *in vivo* report that CTCs roll along blood vessels (Giavazzi et al., 1993b; Aigner et al., 1998; Liu et al., 2018). From our time lapse analysis, we find that this is not a universal CTC behavior. We could not observe any obvious rolling behavior neither *in vitro* nor *in vivo*. (Movie 1-3 and 7-9). This suggests that rolling abilities of CTCs might differ between cancer types or between cancer derived cell lines. This difference in behavior might be due to the expression of distinct cellular adhesion repertoires but also by discrepancies in key biomechanical cellular parameters such as cell stiffness (Wakatsuki et al., 2003), viscosity (Bennett et al., 2018) or membrane tension (Pontes et al., 2017).

In our previous study, we have reported that the initial contact between an arrested CTCs and the endothelium is mediated by a direct interaction between filopodia emanating from the CTC and the closest endothelial cell (Follain et al., 2018a). Recent work also described that the aggressive mouse carcinoma cell line D2A1 produces extensive filopodial like structures which contain adhesive receptors such as integrins αvβ3 and α5β1 (Shibue et al., 2012, 2013). This suggests that the whole adhesive machinery including CD44 could be present at the tip of filopodia of CTC within the blood flow. Such adhesive and highly dynamic structure might be exploited by CTCs to probe the surface of the endothelium, ready to catch their endothelial counterpart to promote CTC arrest. It would be interesting in the future to directly assess the role of such filopodia in CTC arrest endothelium (Follain et al., 2018a).

A previous *in vitro* study has suggested that CTCs engage the laminin contained in the basement membrane below the endothelial layer via integrin α3β1 and α6β1 (Chen et al., 2016b). Interestingly, we also observed that integrin α3β1 mediates CTC arrest in our *in vitro* set up but was not required *in vivo* (Figure 3C and F). One possible explanation between this discrepancy might be that microfluidic set up aiming at culturing endothelial layers to mimic blood vessels *in vitro* form immature and leakier vessel-like structures compared to more impermeable vessels found in *in vivo* models such as the zebrafish embryo. In such microfluidic set up, the cultured endothelial layer might still not be fully impermeable, thus giving opportunity for CTCs to attach to the basal extracellular matrix through filopodia containing integrins. We did not test the involvement α6β1 specifically within our *in vitro* and *in vivo* models, and thus cannot rule out its involvement.

Finally, we observed that fibronectin, the major ligand of integrins αvβ3 and α5β1, is found as deposits at the surface of the endothelial layer both *in vitro* and *in vivo*, in a

process which is flow-dependent (Figure 4). A recent study also suggested that luminal fibronectin is found on the luminal side of liver blood vessels and facilitates CTC arrest in this organ (Barbazán et al., 2017). Past work reported the presence of laminin at the surface of lung blood vessels which correlated with region of CTC arrest (Wang et al., 2004). Fibronectin secretion is a physiologically relevant event as it is secreted on the apical side of epithelial cells of the salivary gland and was shown to be essential during developmental stages such as cleft formation in mouse (Sakai et al., 2003). Fibronectin is also secreted on their surface by endothelial cells, although preferentially basally, and is needed for proper vasculogenesis in the zebrafish embryo (Mana et al., 2016).

It has been shown that cellular exocytosis is driven by the increase in membrane tension (Gauthier et al., 2011). Furthermore, in the zebrafish embryo, we observed an increase in fibronectin deposits in the anterior parts of the dorsal aorta and of the the caudal vein where blood flow is the highest compared to the artero-venous junction (Figure 4F, upper panel) where the lowest flow velocities are measured (Follain et al., 2018a). As the amount of fibronectin deposits scales with blood flow velocities, it is quite tempting to speculate that the shear stress induced by the blood flow might directly promote the secretion of a fibronectin adhesion platform at the luminal side of the endothelial cells.

Altogether, we propose that the first steps of CTC arrest are mediated by a complex interconnection between blood flow and CTC/endothelium adhesion where: (i) blood flow shear stress challenges the finite CTC adhesion force to tune their location of arrest, (ii) CTCs differentially use their adhesion repertoire to arrest and stably adhere to the endothelial layer and (iii) blood flow also tunes CTC arrest by providing a luminal adhesion platform.

AUTHOR CONTRIBUTIONS

N.O. & G.F. performed all experiments and analysis. M.J.G.L and O.L helped with animal experiments. S.H. supervised the study, performed OT experiments and analysis. J.G. conceived the project and supervised the study. NO wrote the paper with input from G.F., S.H., and J.G.

ACKNOWLEDGMENTS

We thank all members of the Goetz Lab for helpful discussions. We are grateful to Tsukasa SHIBUE (MIT) and Robert WEINBERG (MIT) for providing D2A1 cells. We are very grateful to Francesca PERI (EMBL) and Kerstin RICHTER (EMBL) for providing zebrafish embryos. This work has been funded by Plan Cancer (OptoMetaTrap, to J.G. and S.H) and CNRS IMAG'IN (to S.H. and J.G.) and by institutional funds from INSERM and University of Strasbourg. N.O is supported by Plan Cancer. G.F. is supported by La Ligue Contre le Cancer.

REFERENCES

Aigner, S., Ramos, C.L., Hafezi-moghadam, A., Lawrence, M.B., Friederichs, J., Altevogt, P., and Ley, K. (1998). CD24 mediates rolling of breast carcinoma cells on P-selectin. FASEB J *12*, 1241–1251.

Baccelli, I., Schneeweiss, A., Riethdorf, S., Stenzinger, A., Schillert, A., Vogel, V., Klein, C., Saini, M., Bäuerle, T., Wallwiener, M., et al. (2013). Identification of a population of blood circulating tumor cells from breast cancer patients that initiates metastasis in a xenograft assay. Nature Biotechnology *31*, 539–544.

Bano, F., Banerji, S., Howarth, M., Jackson, D.G., and Richter, R.P. (2016). A single molecule assay to probe monovalent and multivalent bonds between hyaluronan and its key leukocyte receptor CD44 under force. Scientific Reports *6*.

Baratchi, S., Almazi, J.G., Darby, W., Tovar-Lopez, F.J., Mitchell, A., and McIntyre, P. (2016). Shear stress mediates exocytosis of functional TRPV4 channels in endothelial cells. Cellular and Molecular Life Sciences *73*, 649–666.

Barbazán, J., Alonso-Alconada, L., Elkhatib, N., Geraldo, S., Gurchenkov, V., Glentis, A., Niel, G. van, Palmulli, R., Fernández, B., Viaño, P., et al. (2017). Liver Metastasis Is Facilitated by the Adherence of Circulating Tumor Cells to Vascular Fibronectin Deposits. Cancer Res *77*, 3431–3441.

Barthel, S.R., Hays, D.L., Yazawa, E.M., Opperman, M., Walley, K.C., Nimrichter, L., Burdick, M.M., Gillard, B.M., Moser, M.T., Pantel, K., et al. (2013). Definition of Molecular Determinants of Prostate Cancer Cell Bone Extravasation. Cancer Research *73*, 942–952.

Bennett, M., Cantini, M., Reboud, J., Cooper, J.M., Roca-Cusachs, P., and Salmeron-Sanchez, M. (2018). Molecular clutch drives cell response to surface viscosity. PNAS *115*, 1192–1197.

Bharadwaj, M., Strohmeyer, N., Colo, G.P., Helenius, J., Beerenwinkel, N., Schiller, H.B., Fässler, R., and Müller, D.J. (2017). αV-class integrins exert dual roles on α5β1 integrins to strengthen adhesion to fibronectin. Nature Communications *8*, 14348.

Boral, D., Vishnoi, M., Liu, H.N., Yin, W., Sprouse, M.L., Scamardo, A., Hong, D.S., Tan, T.Z., Thiery, J.P., Chang, J.C., et al. (2017). Molecular characterization of breast cancer CTCs associated with brain metastasis. Nature Communications *8*.

Campbell, I.D., and Humphries, M.J. (2011). Integrin Structure, Activation, and Interactions. Cold Spring Harbor Perspectives in Biology *3*, a004994–a004994.

Chen, J., Zhou, W., Jia, Q., Chen, J., Zhang, S., Yao, W., Wei, F., Zhang, Y., Yang, F., Huang, W., et al. (2016a). Efficient extravasation of tumor-repopulating cells depends on cell deformability. Scientific Reports *6*, 19304.

Chen, M.B., Lamar, J.M., Li, R., Hynes, R.O., and Kamm, R.D. (2016b). Elucidation of the Roles of Tumor Integrin β1 in the Extravasation Stage of the Metastasis Cascade. Cancer Res *76*, 2513–2524.

Dallas, M.R., Liu, G., Chen, W.-C., Thomas, S.N., Wirtz, D., Huso, D.L., and Konstantopoulos, K. (2012). Divergent roles of CD44 and carcinoembryonic antigen in colon cancer metastasis. FASEB J. *26*, 2648–2656.

Eibl, C., Grigoriu, S., Hessenberger, M., Wenger, J., Puehringer, S., Pinheiro, A.S., Wagner, R.N., Proell, M., Reed, J.C., Page, R., et al. (2012). Structural and Functional Analysis of the NLRP4 Pyrin Domain. Biochemistry *51*, 7330–7341.

Eyles, J., Puaux, A.-L., Wang, X., Toh, B., Prakash, C., Hong, M., Tan, T.G., Zheng, L., Ong, L.C., Jin, Y., et al. (2010). Tumor cells disseminate early, but immunosurveillance limits metastatic outgrowth, in a mouse model of melanoma. Journal of Clinical Investigation *120*, 2030–2039.

Felding-Habermann, B., O'Toole, T.E., Smith, J.W., Fransvea, E., Ruggeri, Z.M., Ginsberg, M.H., Hughes, P.E., Pampori, N., Shattil, S.J., Saven, A., et al. (2001). Integrin activation controls metastasis in human breast cancer. Proceedings of the National Academy of Sciences *98*, 1853–1858.

Follain, G., Osmani, N., Azevedo, A.S., Allio, G., Mercier, L., Karreman, M.A., Solecki, G., Leòn, M.J.G., Lefebvre, O., Fekonja, N., et al. (2018a). Hemodynamic Forces Tune the Arrest, Adhesion, and Extravasation of Circulating Tumor Cells. Developmental Cell *45*, 33-52.e12.

Follain, G., Osmani, N., Fuchs, C., Allio, G., Harlepp, S., and Goetz, J.G. (2018b). Using the Zebrafish Embryo to Dissect the Early Steps of the Metastasis Cascade. In Cell Migration, (Humana Press, New York, NY), pp. 195–211.

Gauthier, N.C., Fardin, M.A., Roca-Cusachs, P., and Sheetz, M.P. (2011). Temporary increase in plasma membrane tension coordinates the activation of exocytosis and contraction during cell spreading. Proceedings of the National Academy of Sciences *108*, 14467–14472.

Giavazzi, R., Foppolo, M., Dossi, R., and Remuzzi, A. (1993a). Rolling and adhesion of human tumor cells on vascular endothelium under physiological flow conditions. Journal of Clinical Investigation *92*, 3038–3044.

Giavazzi, R., Foppolo, M., Dossi, R., and Remuzzi, A. (1993b). Rolling and adhesion of human tumor cells on vascular endothelium under physiological flow conditions. Journal of Clinical Investigation *92*, 3038–3044.

Hanley, W.D., Napier, S.L., Burdick, M.M., Schnaar, R.L., Sackstein, R., and Konstantopoulos, K. (2006). Variant isoforms of CD44 are P- and L-selectin ligands on colon carcinoma cells. FASEB J. *20*, 337–339.

Harper, K.L., Sosa, M.S., Entenberg, D., Hosseini, H., Cheung, J.F., Nobre, R., Avivar-Valderas, A., Nagi, C., Girnius, N., Davis, R.J., et al. (2016). Mechanism of early dissemination and metastasis in Her2+ mammary cancer. Nature *540*, 588–592.

Hiratsuka, S., Goel, S., Kamoun, W.S., Maru, Y., Fukumura, D., Duda, D.G., and Jain, R.K. (2011). Endothelial focal adhesion kinase mediates cancer cell homing to discrete regions of the lungs via E-selectin up-regulation. Proceedings of the National Academy of Sciences *108*, 3725–3730.

Hosseini, H., Obradović, M.M.S., Hoffmann, M., Harper, K.L., Sosa, M.S., Werner-Klein, M., Nanduri, L.K., Werno, C., Ehrl, C., Maneck, M., et al. (2016). Early dissemination seeds metastasis in breast cancer. Nature *540*, 552–558.

Humphries, J.D. (2006). Integrin ligands at a glance. Journal of Cell Science *119*, 3901–3903.

Huveneers, S., Truong, H., Fassler, R., Sonnenberg, A., and Danen, E.H.J. (2008). Binding of soluble fibronectin to integrin 5 1 - link to focal adhesion redistribution and contractile shape. Journal of Cell Science *121*, 2452–2462.

Klemke, M., Weschenfelder, T., Konstandin, M.H., and Samstag, Y. (2007). High affinity interaction of integrin alpha4beta1 (VLA-4) and vascular cell adhesion molecule 1 (VCAM-1) enhances migration of human melanoma cells across activated endothelial cell layers. J. Cell. Physiol. *212*, 368–374.

Köhler, K., Xiong, S., Brzostek, J., Mehrabi, M., Eissmann, P., Harrison, A., Cordoba, S.-P., Oddos, S., Miloserdov, V., Gould, K., et al. (2010). Matched sizes of activating and inhibitory receptor/ligand pairs are required for optimal signal integration by human natural killer cells. PLoS ONE *5*, e15374.

Kong, F., García, A.J., Mould, A.P., Humphries, M.J., and Zhu, C. (2009). Demonstration of catch bonds between an integrin and its ligand. The Journal of Cell Biology *185*, 1275–1284.

Kong, F., Li, Z., Parks, W.M., Dumbauld, D.W., García, A.J., Mould, A.P., Humphries, M.J., and Zhu, C. (2013). Cyclic Mechanical Reinforcement of Integrin-Ligand Interactions. Molecular Cell *49*, 1060–1068.

Laferrière, J., Houle, F., Taher, M.M., Valerie, K., and Huot, J. (2001). Transendothelial Migration of Colon Carcinoma Cells Requires Expression of E-selectin by Endothelial Cells and Activation of Stress-activated Protein Kinase-2 (SAPK2/p38) in the Tumor Cells. Journal of Biological Chemistry *276*, 33762–33772.

Laferrière, J., Houle, F., and Huot, J. (2004). Adhesion of HT-29 colon carcinoma cells to endothelial cells requires sequential events involving E-selectin and integrin beta4. Clin. Exp. Metastasis *21*, 257–264.

Liu, T.-L., Upadhyayula, S., Milkie, D.E., Singh, V., Wang, K., Swinburne, I.A., Mosaliganti, K.R., Collins, Z.M., Hiscock, T.W., Shea, J., et al. (2018). Observing the cell in its native state: Imaging subcellular dynamics in multicellular organisms. Science *360*, eaaq1392.

Mana, G., Clapero, F., Panieri, E., Panero, V., Böttcher, R.T., Tseng, H.-Y., Saltarin, F., Astanina, E., Wolanska, K.I., Morgan, M.R., et al. (2016). PPFIA1 drives active α5β1 integrin recycling and controls fibronectin fibrillogenesis and vascular morphogenesis. Nature Communications *7*, 13546.

McEver, R.P., and Zhu, C. (2010). Rolling Cell Adhesion. Annual Review of Cell and Developmental Biology *26*, 363–396.

Obenauf, A.C., and Massagué, J. (2015). Surviving at a Distance: Organ-Specific Metastasis. Trends in Cancer *1*, 76–91.

Pontes, B., Monzo, P., Gole, L., Roux, A.-L.L., Kosmalska, A.J., Tam, Z.Y., Luo, W., Kan, S., Viasnoff, V., Roca-Cusachs, P., et al. (2017). Membrane tension controls adhesion positioning at the leading edge of cells. J Cell Biol *216*, 2959–2977.

Rahn, J.J., Chow, J.W., Horne, G.J., Mah, B.K., Emerman, J.T., Hoffman, P., and Hugh, J.C. (2005). MUC1 mediates transendothelial migration in vitro by ligating endothelial cell ICAM-1. Clin. Exp. Metastasis *22*, 475–483.

Reymond, N., Im, J.H., Garg, R., Vega, F.M., Borda d'Agua, B., Riou, P., Cox, S., Valderrama, F., Muschel, R.J., and Ridley, A.J. (2012). Cdc42 promotes transendothelial migration of cancer cells through β1 integrin. The Journal of Cell Biology *199*, 653–668.

Reymond, N., d'Água, B.B., and Ridley, A.J. (2013). Crossing the endothelial barrier during metastasis. Nature Reviews Cancer *13*, 858–870.

Rhim, A.D., Mirek, E.T., Aiello, N.M., Maitra, A., Bailey, J.M., McAllister, F., Reichert, M., Beatty, G.L., Rustgi, A.K., Vonderheide, R.H., et al. (2012). EMT and Dissemination Precede Pancreatic Tumor Formation. Cell *148*, 349–361.

Roca-Cusachs, P., Gauthier, N.C., del Rio, A., and Sheetz, M.P. (2009). Clustering of α5β1 integrins determines adhesion strength whereas αvβ3 and talin enable mechanotransduction. Proceedings of the National Academy of Sciences *106*, 16245–16250.

Sakai, T., Larsen, M., and Yamada, K.M. (2003). Fibronectin requirement in branching morphogenesis. Nature *423*, 876–881.

Shea, D.J., Wirtz, D., Stebe, K.J., and Konstantopoulos, K. (2015). Distinct kinetic and mechanical properties govern mucin 16- and podocalyxin-mediated tumor cell adhesion to E- and L-selectin in shear flow. Oncotarget *6*, 24842–24855.

Shibue, T., Brooks, M.W., Inan, M.F., Reinhardt, F., and Weinberg, R.A. (2012). The Outgrowth of Micrometastases Is Enabled by the Formation of Filopodium-like Protrusions. Cancer Discovery *2*, 706–721.

Shibue, T., Brooks, M.W., and Weinberg, R.A. (2013). An Integrin-Linked Machinery of Cytoskeletal Regulation that Enables Experimental Tumor Initiation and Metastatic Colonization. Cancer Cell *24*, 481–498.

Stoletov, K., Kato, H., Zardouzian, E., Kelber, J., Yang, J., Shattil, S., and Klemke, R. (2010). Visualizing extravasation dynamics of metastatic tumor cells. Journal of Cell Science *123*, 2332–2341.

Tremblay, P.-L., Huot, J., and Auger, F.A. (2008). Mechanisms by which E-Selectin Regulates Diapedesis of Colon Cancer Cells under Flow Conditions. Cancer Research *68*, 5167–5176.

Wakatsuki, T., Wysolmerski, R.B., and Elson, E.L. (2003). Mechanics of cell spreading: role of myosin II. Journal of Cell Science *116*, 1617–1625.

Wang, H., Fu, W., Im, J.H., Zhou, Z., Santoro, S.A., Iyer, V., DiPersio, C.M., Yu, Q.-C., Quaranta, V., Al-Mehdi, A., et al. (2004). Tumor cell α3β1 integrin and vascular laminin-5 mediate pulmonary arrest and metastasis. J Cell Biol *164*, 935–941.

LEGENDS

Figure 1 – CD44, ITGB3 and ITGB1 are involved in CTC arrest/adhesion but only ITGB1 is required for stable adhesion *in vitro*. (A) Scheme of the experimental approach for the microfluidic CTC arrest assay. (B) D2A1 cells were transfected with indicated siRNAs. Representative western blot images from 72h extract are shown in the upper panel. The graphs show the mean ± S.D. of 3 independent experiments. (C) D2A1 were perfused into microfluidic channels

containing a confluent monolayer of endothelial cells (HUVEC) for 2 min at the indicated speeds. The number of cells adhered is quantified and normalized to the number of cells adherent at the lowest perfusion speed (100 µm/s). The graph shows the mean ± S.D. (left) and mean ± S.D. (right) of 14 independent experiments. (D) Upper panel: time projection of 2 min perfusion of D2A1 cells at 100 µm/s showing arrested cells. Lower panel: time projection of 2 min wash step (perfusion of medium at 400 µm/s) showing transiently arrested cells (metastable, red) or stably arrested cells (stable, green). Related to movie 1. (E) D2A1 cells were transfected with indicated siRNAs and perfused into microfluidic channels containing a confluent monolayer of endothelial cells (HUVEC). The number of cells adhered normalized to siCTL was quantified (left) and the ratio of stably adhering cells was measured (right). The graph shows the mean ± S.E.M. (left) and mean ± S.D. (right) of 6 independent experiments. Related to movie 2 and 3. (F) Scheme of the experimental approach for the microfluidic CTC stable adhesion assay. (G) D2A1 cells were transfected with indicated siRNAs, perfused into microfluidic channels containing a confluent monolayer of endothelial cells (HUVEC) and left to attach to the endothelial layer without flow for 5 min. Attached cells were then trapped into the optical tweezer beam and the stage was moved away using the piezo stage. The graph shows the mean ± S.D. of 3 independent experiments. Related to movies 4 to 6.

Figure 2 – CD44 and ITGB3 are involved in CTC arrest while ITGB1 is required for stable adhesion *in vivo*. (A) Scheme of the experimental approach for the *in vivo* CTC arrest assay. (B-C) D2A1 cells were transfected with indicated siRNAs and microinjected into the duct of Cuvier of 3 dpf *Tg(Fli1a:EGFP)* embryos. Cell arrests were live imaged at 4 fps for 5 min immediately after injection. (B) The graphs show the mean ± S.D. of 3 independent experiments. (C) Time projection of representative embryo injected with cells transfected with indicated siRNAs. The color code shows the arrest time of CTCs. Related to movies 7 to 9. (F-G) D2A1 cells were transfected with indicated siRNAs and microinjected into the duct of Cuvier of 2 dpf *Tg(Fli1a:EGFP)* embryos. Cell adhesion pattern was imaged 3h after injection. The heatmaps show the quantification of the number and location of stably arrested CTCs at 3 hpi in the caudal plexus of embryo injected with indicated siRNAs. The graphs show the mean ± S.D. of 5 independent experiments.

Figure 3 – ITGA5 phenocopies ITGB1 role in CTC adhesion to endothelial cells. (A) D2A1 cells were transfected with indicated siRNAs. The expression of the genes of interest were measured using RT-qPCR. The graph shows the mean ± S.E.M. of at least 3 independent experiments. (B-D) D2A1 cells were transfected with indicated siRNAs and perfused into microfluidic channels containing a confluent monolayer of endothelial cells (HUVEC). The number of cells adhered normalized to siCTL was quantified (left) and the ratio of stably adhering cells was measured (right). The graph shows the mean ± S.E.M. (left) and mean ± S.D. (right) of at least 4 independent experiments. (E-G) Quantification using heatmapping of the number and location of stably arrested CTCs at 3 hpi in the caudal plexus of embryo injected with cells transfected with indicated siRNAs. The graphs show the mean ± S.E.M. of 4 independent experiments.

Figure 4 – Flow drives the formation of luminal FN deposits. (A) HUVEC cells were grown to confluency in microfluidic channels and subjected to either no flow or a laminar flow of 400 µm/s for 16h. Cells are immunostained for fibronectin (green), actin (red) and nucleus (blue). A y-projection of 35 single representative transversal confocal slices is shown in the bottom panel XZ. (B) The ratio of HUVEC cells with fibronectin (FN) deposits was quantified. The graphs show the mean ± S.D. of 3 independent experiments. (C) HUVEC cells were grown to confluency in microfluidic channels and subjected to either no flow or a laminar flow of 400 µm/s for 16h. Fibronectin (FN) expression was then quantified. A representative western blot image is shown in the upper panel The graphs show the mean ± S.D. of 5 independent experiments. (D) Scheme of the experimental approach for the *in vivo* luminal FN quantification. (E) 2 dpf *Tg(Fli1a:EGFP)* embryos were either untreated (NT) or treated for 2h with vehicle (EtOH) or lidocain at 640 µM (Lido). Embryos were then processed for endogenous fibronectin immunostaining and the presence of fibronectin deposits was assessed. The graphs show the mean ± S.D. of 6 independent experiments. (F) Representative embryos were imaged using light sheet microscopy (SPIM).

Figure S1 – siRNAs knockdown validation 96h after transfection. D2A1 cells were transfected with control or anti-CD44 siRNAs. Protein extracts were prepared

96h later and immunoblotted against CD44 or GAPDH. The graph shows the mean ± S.D. of 3 independent experiments.

Movie 1 – Live adhesion assay. D2A1 cells were transfected with control siRNAs. 72h later, cells were detached and perfused into microfluidic channels for 2 min at the indicated speeds. The movie is acquired at 24 fps and displayed at 72 fps. Related to Figure 1E.

Movie 2 – Live adhesion movie of siCTL, siCD44 and siITGB1 transfected cells. D2A1 cells were transfected with control, anti-CD44 or anti-ITGB1 siRNAs. 72h later, cells were detached and perfused into microfluidic channels. The movie shows in parallel the perfusion of the three conditions at 100 µm/s. The movie is acquired at 24 fps and displayed at 72 fps. Related to Figure 1E.

Movie 3 – Live adhesion movie of siCTL and siITGB3 transfected cells. D2A1 cells were transfected with control or anti-ITGB3 siRNAs. 72h later, cells were detached and perfused into microfluidic channels. The movie shows in parallel the perfusion of the two conditions at 100 µm/s. The movie is acquired at 24 fps and displayed at 72 fps. Related to Figure 1E.

Movie 4 – CD44 is not involved in stable adhesion *in vitro*. D2A1 cells were transfected with control siRNAs or anti-CD44. 72h later, cells were detached and perfused into microfluidic channels containing a confluent monolayer of endothelial cells (HUVEC) and left to attach to the endothelial layer without flow for 5 min. Attached cells were then trapped into the optical tweezer beam and the stage was moved away using the piezo stage. The movie is acquired at 24 fps and displayed at 72 fps. Related to Figure 1G.

Movie 5 – ITGB3 is involved in stable adhesion *in vitro*. D2A1 cells were transfected with control siRNAs or anti-ITGB3. 72h later, cells were detached and perfused into microfluidic channels containing a confluent monolayer of endothelial cells (HUVEC) and left to attach to the endothelial layer without flow for 5 min.

Attached cells were then trapped into the optical tweezer beam and the stage was moved away using the piezo stage. The movie was acquired at 24 fps and displayed at 72 fps. Related to Figure 1G.

Movie 6 – ITGB1 is involved in stable adhesion *in vitro*. D2A1 cells were transfected with control siRNAs or anti-ITGB1. 72h later, cells were detached and perfused into microfluidic channels containing a confluent monolayer of endothelial cells (HUVEC) and left to attach to the endothelial layer without flow for 5 min. Attached cells were then trapped into the optical tweezer beam and the stage was moved away using the piezo stage. The movie was acquired at 24 fps and displayed at 72 fps. Related to Figure 21G.

Movie 7 – CD44 is involved in CTC arrest/early adhesion *in vivo*. D2A1 cells were transfected with control or anti-CD44 siRNAs. 72h later, cells were detached and microinjected into the duct of Cuvier of 2 dpf *Tg(Fli1a:EGFP)* embryos. Cell arrests was live imaged at 4 fps for 2,5 min immediately after injection. The movie is displayed at 80 fps. Related to Figure 2A-C.

Movie 8 – ITGB3 is involved in CTC arrest/early adhesion *in vivo*. D2A1 cells were transfected with control or anti-ITGB1 siRNAs. 72h later, cells were detached and microinjected into the duct of Cuvier of 2 dpf *Tg(Fli1a:EGFP)* embryos. Cell arrests was live imaged at 4 fps for 2,5 min immediately after injection. The movie is displayed at 80 fps. Related to Figure 2A-C.

Movie 9 – ITGB1 is involved in CTC arrest/early adhesion *in vivo*. D2A1 cells were transfected with control or anti-ITGB1 siRNAs. 72h later, cells were detached and microinjected into the duct of Cuvier of 2 dpf *Tg(Fli1a:EGFP)* embryos. Cell arrests was live imaged at 4 fps for 2,5 min immediately after injection. The movie is displayed at 80 fps. Related to Figure 2A-C.

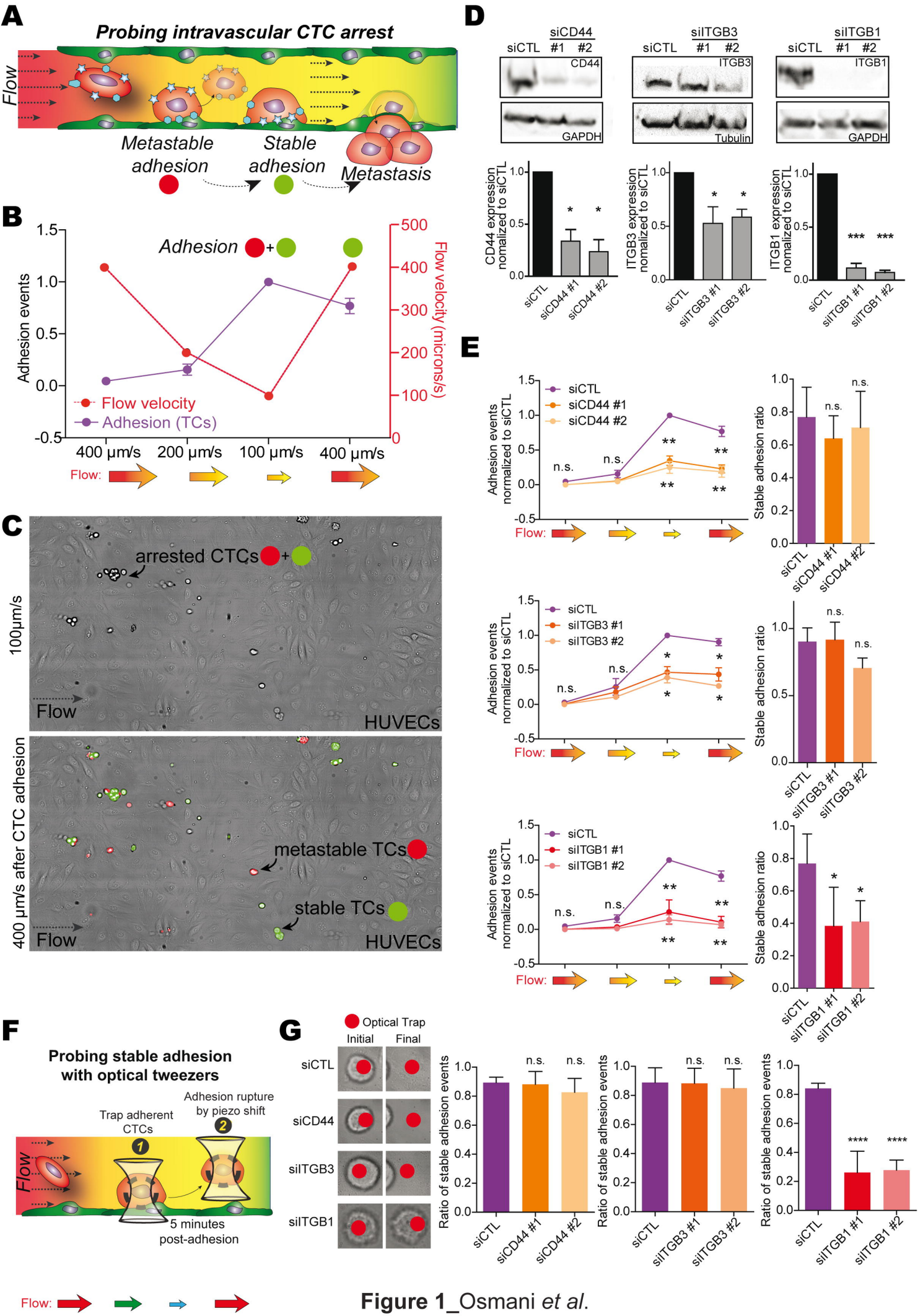

Figure 1_Osmani *et al.*

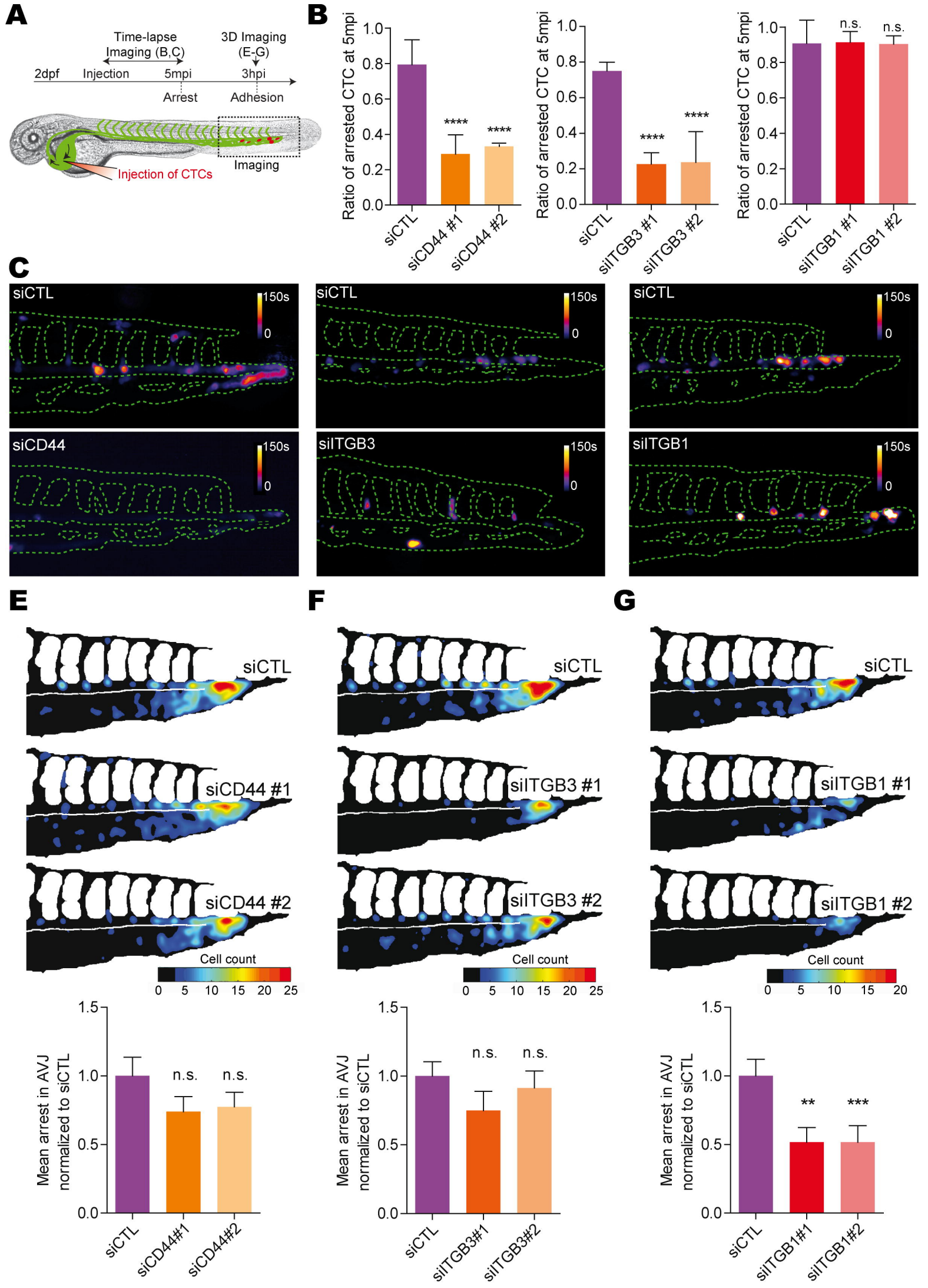

Figure 2_Osmani *et al.*

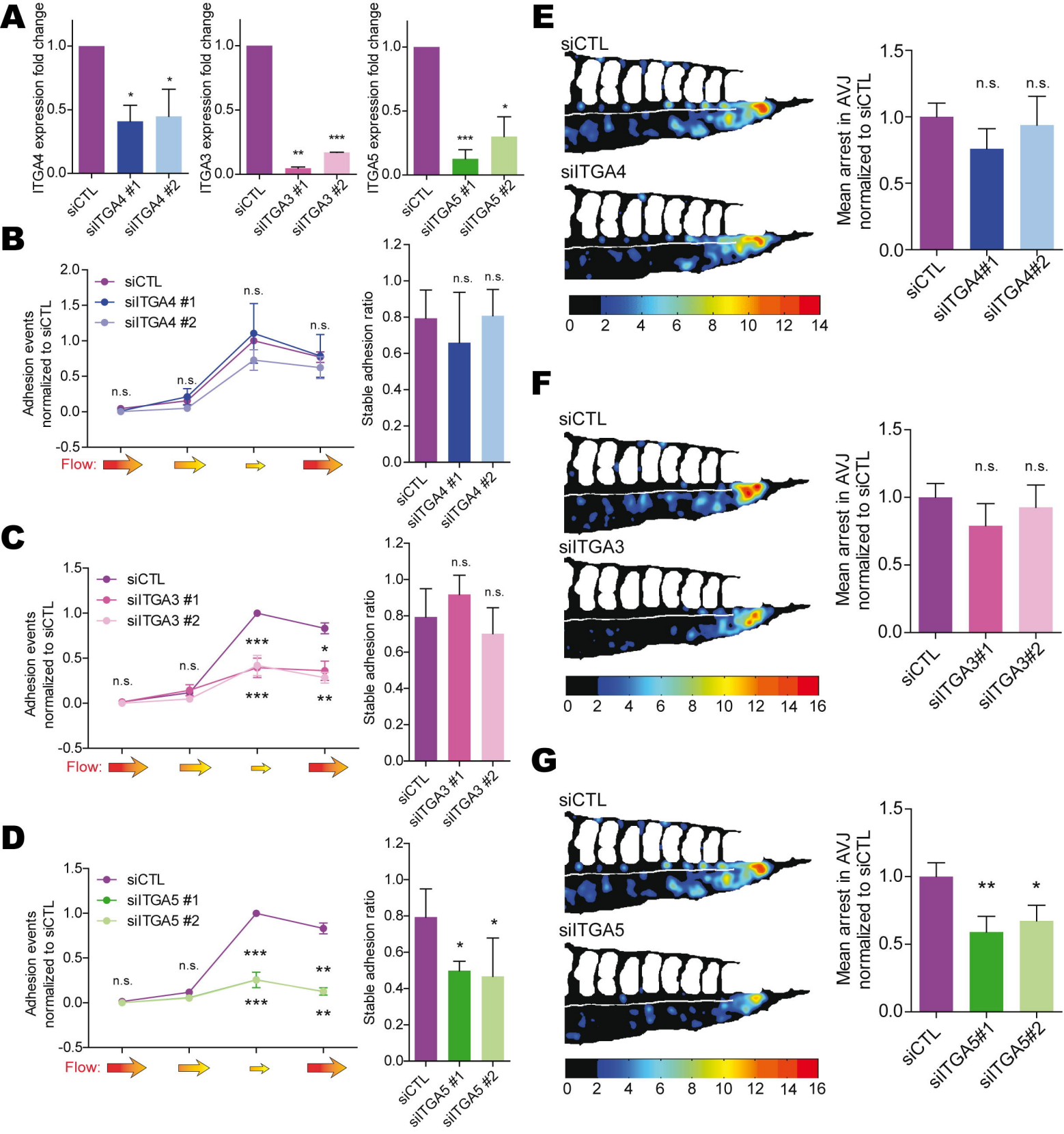

Figure 3_Osmani *et al*.

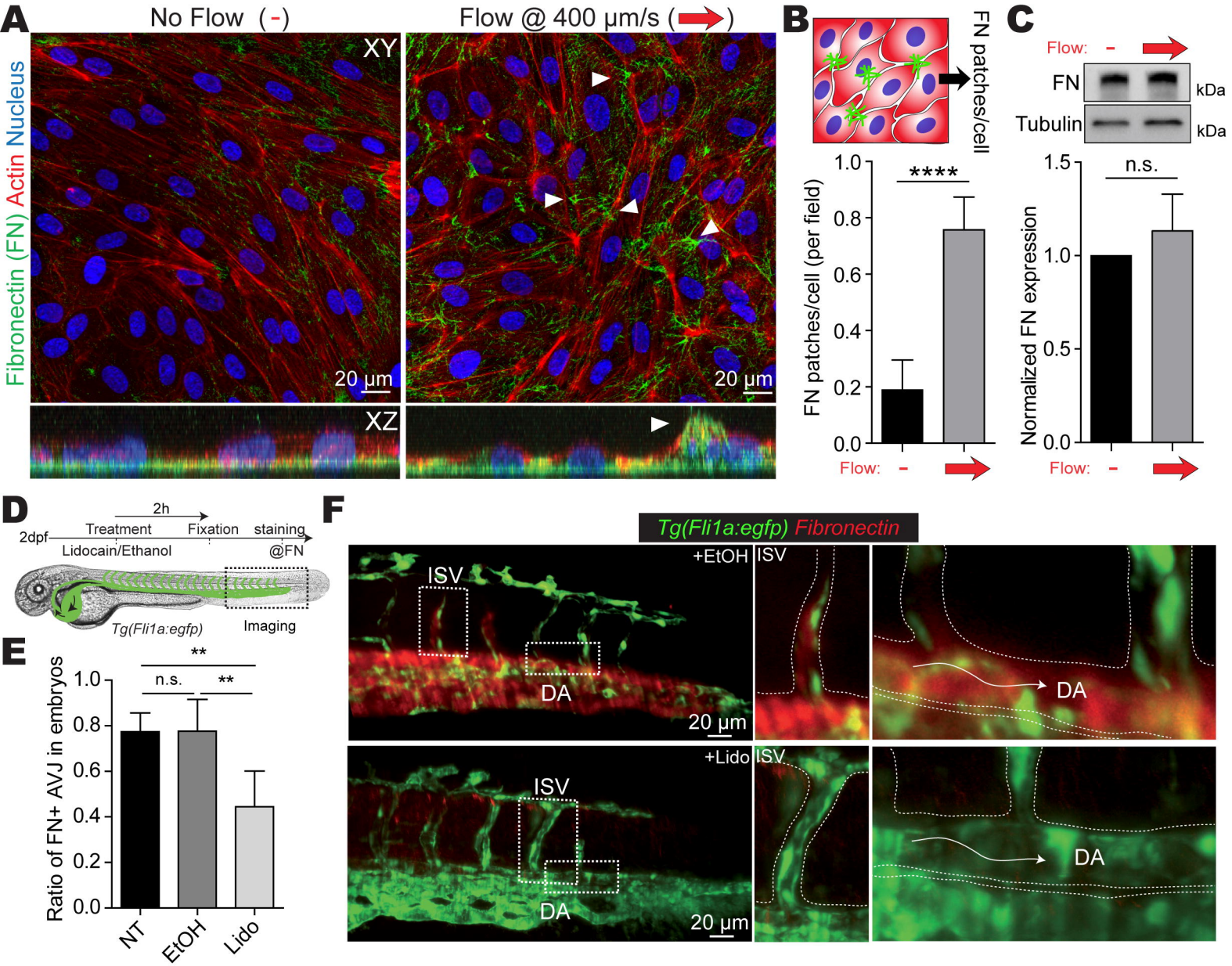

Figure 4_Osmani *et al.*

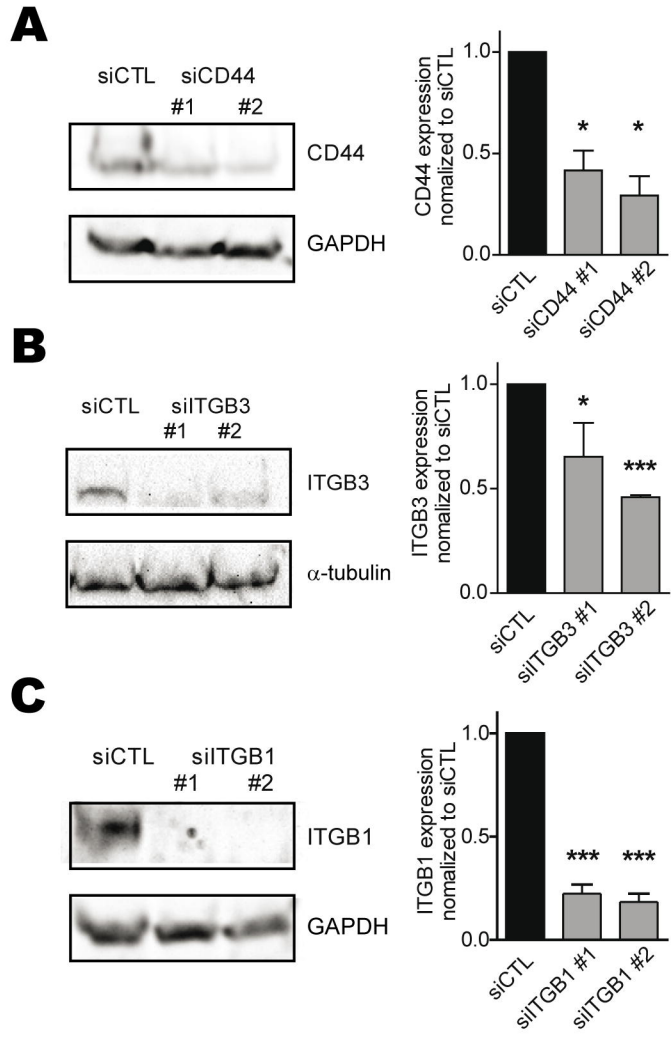

Figure S1_Osmani *et al*.